DIFFUSION

The electrical characteristics of the active devices in an integrated circuit (IC) are largely determined by the placement

and distribution of dopants. Dopant atoms are introduced during front-end processing at various stages, mostly using ion implantation, and they diffuse during the subsequent thermal treatments that create, e.g., the gate oxide. The final configuration is the result of a complex interaction of dopants with themselves, the native point defects, processing-induced damage, and the interfaces to various films, such as oxides, nitrides, and silicides. Accurate prediction and control of the 3-dimensional dopant distribution is of extreme importance to IC manufacturing and the subject of an intense effort by industry and academia.

DIFFUSION IN SOLIDS

Phenomenological Description

Diffusion is the spontaneous mass transport that occurs because of a chemical potential gradient. That gradient may be due to changes in concentration only, in which case Fick's first law relates the mass-flux of the moving species, $\vec{J}$, with the spatial variation of the concentration c as

$$\vec{J} = -\boldsymbol{D}\vec{\nabla}c \tag{1}$$

In general, $\boldsymbol{D}$ is a tensor of rank 2 and each of its elements depends on concentration. For sufficiently low concentrations and for isotropic media, $\boldsymbol{D}$ can be taken as a scalar constant, called *diffusion coefficient.* Taking the continuity equation, that is, mass conservation, into account yields Fick's second law:

$$\frac{\partial c}{\partial t} = \vec{\nabla}(D\vec{\nabla}c) \tag{2}$$

where t denotes the time. If D is concentration-independent, then Eq. (2) simplifies in one dimension to

$$\frac{\partial c}{\partial t} = D\frac{\partial^2 c}{\partial x^2} \tag{3}$$

where x is the spatial coordinate along which diffusion occurs. It has an analytical solution given by

$$c(x,t) = \frac{1}{2\sqrt{\pi Dt}}\int_{-\infty}^{\infty} c(\xi,0)e^{-(x-\xi)^2/2Dt}d\xi \tag{4}$$

which can easily be evaluated numerically for arbitrary starting concentration profiles $c(\xi, 0)$. The quantity $\Lambda = \sqrt{Dt}$ is called the diffusion length and is commonly used as a rough estimate of the amount of diffusion that occurred. Determining Λ^2 as a function of diffusion time has to yield a linear dependence on t. Violation of this condition indicates that D is not concentration- and/or time-independent and that Eq. (4) does not apply.

Selected Solutions of the Concentration-Independent Diffusion Equation

Fixed Surface Concentration. In this case [Figs. 1(a) and 1(b)]

$$c(x,t) = c_s\mathrm{erfc}\left(\frac{x}{2\sqrt{Dt}}\right) \tag{5}$$

where c_s is the surface concentration. The total amount per unit area that has diffused is given by

$$N_{2D} = \frac{2c_s}{\sqrt{\pi}}\sqrt{Dt} \tag{6}$$

An example is the annealing of a doped epitaxial film when the solubility and diffusivity of the dopant in the film is much higher than in the substrate.

Infinite Source. Assume for the concentration at $t = 0$

$$c(x,0) = \begin{cases} c_0 & \text{if } x < 0 \\ 0 & \text{if } x > 0 \end{cases} \tag{7}$$

then after diffusion

$$c(x,t) = \frac{c_0}{2}\mathrm{erfc}\left(\frac{x}{2\sqrt{Dt}}\right) \tag{8}$$

The solution is formally identical to that for fixed surface concentration, except for a factor $\frac{1}{2}$ in concentration [Figs. 1(a–b)]. An example is the annealing of a doped epitaxial film with a thickness much larger than the diffusion distance.

Gaussian Profile. To first order, ion implanted profiles can be described by a range R_p, and longitudinal straggle σ_p, with the concentration after implant given by a Gaussian profile [Figs. 1(c–d)]

$$c(x,0) = \frac{N_{2D}}{\sigma\sqrt{2\pi}}e^{-(x-R_p)^2/2\sigma^2} \tag{9}$$

where N_{2D} is the implant dose in atoms per unit area, and $\sigma = \sigma_p$. The full-width-at-half-maximum is given by $2\sigma_p\sqrt{2\ln 2}$. Because of the mathematical properties of a Gaussian and the structure of Eq. (4), the profile after diffusion is again a Gaussian but now with

$$\sigma^2 = \sigma_p^2 + 2Dt \tag{10}$$

This result also applies to buried layers ("delta-doping"), provided that their width before diffusion is much smaller than the diffusion length (1).

General Solutions. More complicated cases, including certain types of concentration dependence of D and nonisotropic media, have been treated in Ref. 2. However, today, the availability of desktop workstations and the numerical analysis capabilities of process simulator programs, such as PROPHET (3), SUPREM4 (4), or FLOOPS (5) have made algebraic calculation of diffusion profiles obsolete beyond the few simple cases discussed above.

Atomistic Description

Diffusion Mechanisms. On a microscopic level diffusion in solids takes place through a series of atomic jumps with [Fig. 2(a–c)] or without [Fig. 2(d)] involvement of native defects. In all cases, movement of an atom requires that a certain energy

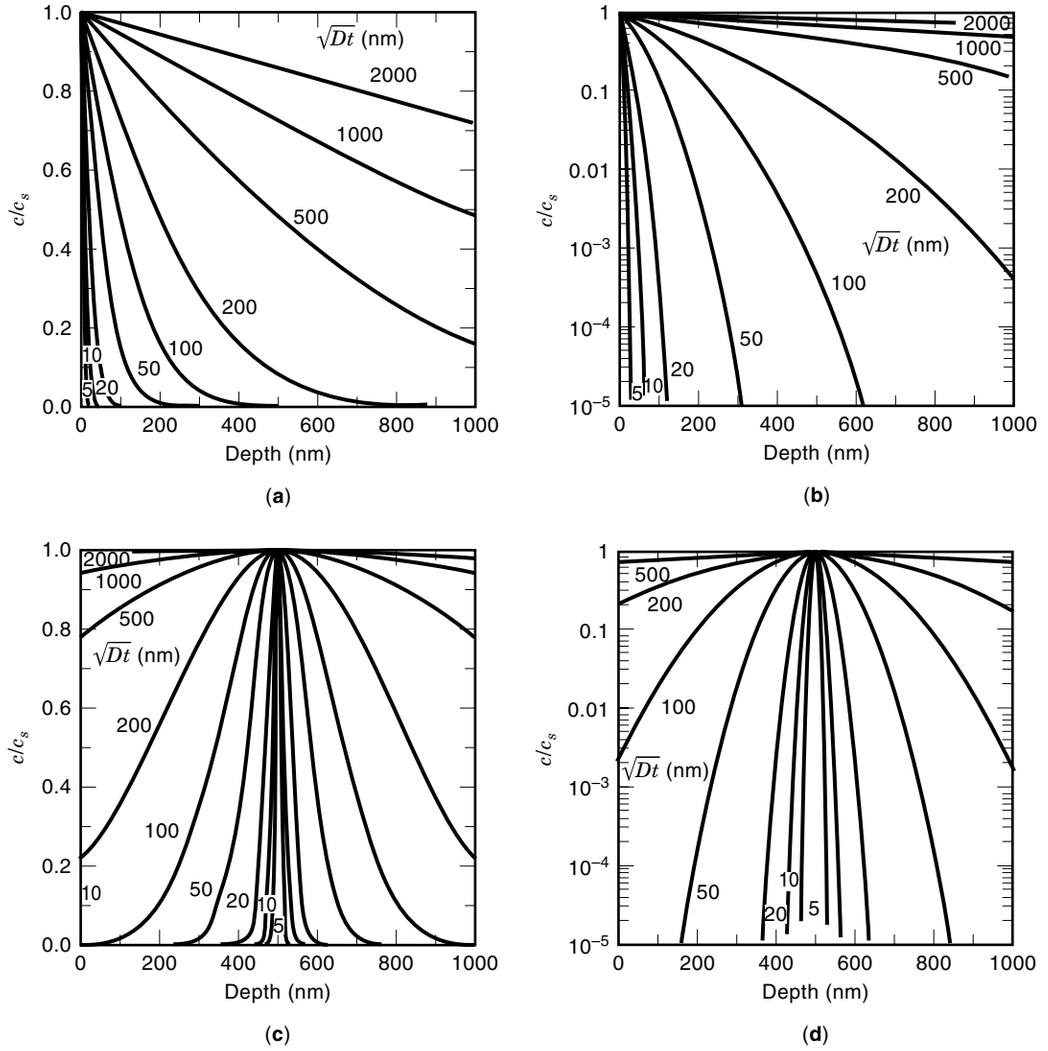

Figure 1. Selected solutions of the diffusion equation in one dimension for a concentration-independent diffusion coefficient: (a–b) fixed surface concentration, (c–d) Gaussian profile.

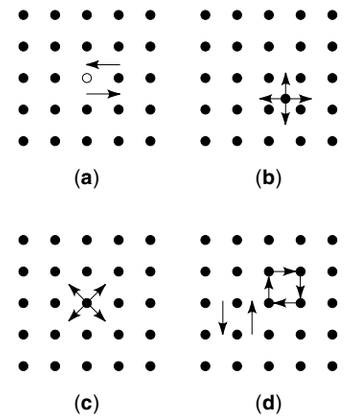

Figure 2. Schematic of diffusion mechanisms in a 2-dimensional square lattice. (a) vacancy mechanism; (b) interstitial mechanism; (c) interstitialcy mechanism; (d) place and ring exchange. Filled circles represent impurity atoms, open circles represent host atoms, and the open square stands for a missing host atom (vacancy).

barrier be overcome (Fig. 3). The number of successful jumps per unit time v_s, is therefore

$$v_s = ve^{-G_m/kT} \tag{11}$$

where v is the number of attempted jumps per unit time (attempt frequency) and equal to the Debye frequency; G_m is the Gibbs free energy of migration; and T is the temperature. The Einstein diffusion equation holds for the mean-square displacement $\langle \Delta \vec{x}^2 \rangle$, of the resulting random walk (Brownian motion), that is

$$\langle \Delta \vec{x}^{\,2} \rangle = 2td \tag{12}$$

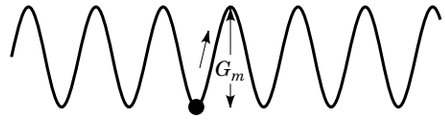

Figure 3. Potential energy diagram (schematic) of an atom in a lattice.

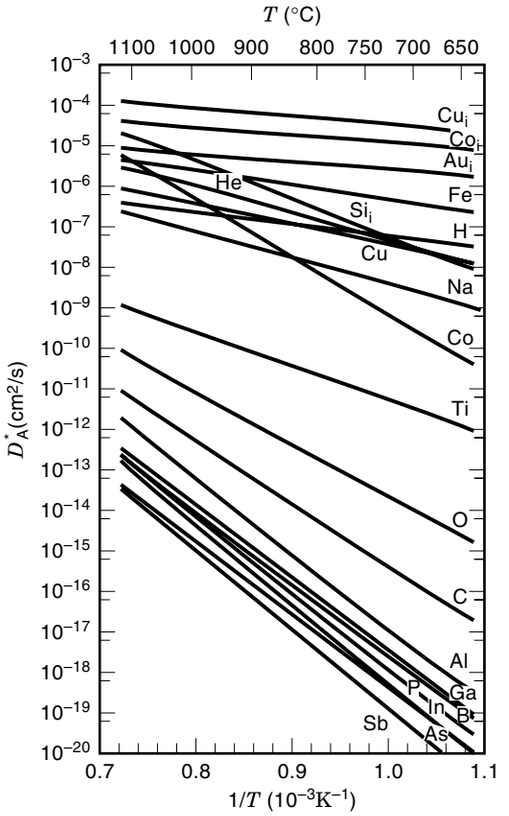

Figure 4. Diffusion coefficients in Si.

where d is the diffusivity of the migrating entity, which in the case of defect-mediated diffusion does not take the creation of the migrating defect into account. We also have

$$\langle \Delta \vec{x}^2 \rangle = f\alpha v_s t \lambda^2 \tag{13}$$

where f represents the correlation factor ($f = 1$ for uncorrelated jumps such as those occurring by means of the interstitial mechanism); α the symmetry of the lattice ($\alpha = \frac{1}{6}$ for a fcc lattice); and λ the distance of a single jump ($\sqrt{3}/4a_0$ for a next-nearest-neighbor jump in an fcc crystal); a_0 is the lattice constant. Hence the diffusion coefficient of the moving species for a particular diffusion mechanism can be written as

$$d = d_0 e^{-H_m/kT} \tag{14}$$

with the prefactor d_0 given by

$$d_0 = f\alpha\lambda^2 v_0 e^{S_m/kT} \tag{15}$$

and H_m and S_m as the enthalpy and entropy of migration, respectively.

Assuming thermal equilibrium and the absence of charge effects, the macroscopic diffusion coefficient is given by

$$D = \begin{cases} dC_m/C & \text{for defect-mediated diffusion} \\ d & \text{for place or ring exchange} \end{cases} \tag{16}$$

where C_m/C is the migrating fraction. Since C_m is of the form $C_{m,0}\, exp(-H_m/kT)$, D is of the general form

$$D = D_0 e^{-H/kT} \tag{17}$$

with H the enthalpy of diffusion. In principle, the total diffusion coefficient is the sum of the contributions from all diffusion mechanisms. Typically, however, one mechanism dominates. Diffusion coefficients in Si, polycrystalline Si, and SiO_2 have been tabulated in Ref. 6; selected coefficients in intrinsic Si are shown in Fig. 4. A more recent compilation, which also includes diffusion coefficients in III–V compounds, can be found in Ref. 7.

THE STANDARD MODEL OF POINT-DEFECT MEDIATED DIFFUSION

The common dopants in Si all diffuse by means of intrinsic point defects (Si self-interstitials and Si vacancies) (8). While the phenomenological treatment above describes diffusion adequately in thermal equilibrium and for concentrations below the intrinsic carrier concentration, these conditions quite often do not exist in practice. Strictly, Fick's law [Eq. (1)] only applies to the migrating entity. Point defects, X, exist in various charge states i, so that for a substitutional atom

$$A^{(\pm 1)} + X^{(i\mp 1)} \leftrightarrow AX^{(i)} \tag{18}$$

where the top of the double sign applies to n-type material (donors) and the bottom to p-type (acceptors). Note that the standard model of dopant diffusion in Si does not make any assumptions about the precise mechanism of diffusion except that the interaction can be written in the form of the rate equation Eq. (18). The total flux of complexes is then

$$\vec{J} = \sum_{X,i} -d_{AX^{(i)}} \vec{\nabla} C_{AX^{(i)}} + i\mu_{AX^{(i)}} C_{AX^{(i)}} \vec{E} \tag{19}$$

The summation extends over all defects and charge states. In addition to Fickian diffusion, a second term has been added in Eq. (19) that represents the drift of the (charged) dopant-defect complexes in the electric field $\vec{E}$: $\mu_{AX^{(i)}}$ is their mobility. The internal field is related to the Fermi level ϵ_F, and the carrier concentration m by

$$\vec{E} = -\frac{1}{q}\vec{\nabla}\epsilon_F = \mp\frac{kT}{q}\vec{\nabla}\ln\frac{m}{n_{\mathrm{INT}}} \tag{20}$$

Here q is the elementary charge; $m = n$ for donors and $m = p$ for acceptors; n and p are the electron and hole concentrations respectively; and the intrinsic electron concentration is denoted by n_{INT} (given in Ref. 9). Further, Einstein's relation holds

$$\mu_{AX^{(i)}} = \frac{q}{kT} d_{AX^{(i)}} \tag{21}$$

Experimentally, one can only measure the total concentration of dopant atoms C_A, and the corresponding diffusivity D_A. In terms of these accessible parameters

$$\vec{J} = -D_A \vec{\nabla} C_A \tag{22}$$

If all dopant atoms are electrically active, that is, no precipitation or other losses have occurred, then charge neutrality requires that

$$\frac{m}{n_{\mathrm{INT}}} = \frac{C_A}{2n_{\mathrm{INT}}} + \left[\frac{C_A^2}{4n_{\mathrm{INT}}^2} + 1\right]^{1/2} \tag{23}$$

For local equilibrium (generally, a good assumption, see Ref. 10) the mass action law yields from Eq. (18)

$$C_A C_{X(i\mp1)} = k_{X,i} C_{AX(i)} \tag{24}$$

where $k_{X,i}$ is a constant, and thus

$$\begin{aligned} C_A \vec{\nabla} C_{X(i\mp1)} + C_{X(i\mp1)} \vec{\nabla} C_A &= k_{X,i} \vec{\nabla} C_{AX(i)} \\ &= \frac{C_A C_{X(i\mp1)}}{C_{AX(i)}} \vec{\nabla} C_{AX(i)} \end{aligned} \tag{25}$$

Hence Eq. (19) becomes

$$\vec{J} = -\sum_{X,i} d_{AX(i)} \left[\frac{C_{AX(i)}}{C_{X(i\mp1)}} \vec{\nabla} C_{X(i\mp1)} + \frac{C_{AX(i)}}{C_A} \vec{\nabla} C_A \pm i \frac{C_{AX(i)} \vec{\nabla} C_A}{2n_{\mathrm{INT}} \sqrt{C_A^2/(4n_{\mathrm{INT}}^2) + 1}} \right] \tag{26}$$

The concentration of defects in various charge states can be written as (10)

$$\frac{C_{X(i)}}{C_{X(i)}^{INT}} = \left[\frac{m}{n_{\mathrm{INT}}}\right]^{\mp i} \tag{27}$$

where $C_{X^{(i)}}^{INT}$ is the concentration under intrinsic conditions. Thus

$$\frac{C_{AX(i)}}{C_{X(i\mp1)}} \vec{\nabla} C_{X(i\mp1)} = \mp(i \mp 1) \frac{C_{AX(i)}}{C_A} (h-1) \vec{\nabla} C_A \tag{28}$$

where

$$h \equiv 1 + \frac{C_A}{2n_{\mathrm{INT}} \sqrt{C_A^2/(4n_{\mathrm{INT}}^2) + 1}} \tag{29}$$

Inserting Eqs. (24), (27), and (28) into (26) and collecting the various terms gives

$$\vec{J} = -\sum_{X,i} h \frac{d_{AX(i)}}{k_{X,i}} C_{X(i\mp1)}^{INT} \left[\frac{m}{n_{\mathrm{INT}}}\right]^{\mp i+1} \vec{\nabla} C_A \tag{30}$$

We now define an equilibrium diffusion coefficient of a pair in a particular charge state by

$$D_{AX(i\mp1)}^{*} = \frac{d_{AX(i)} C_{X(i\mp1)}^{INT*}}{k_{X,i}} \tag{31}$$

and obtain, by comparison of Eq. (30) with (22), the equilibrium diffusion coefficient of the dopant A under extrinsic conditions as

$$D_A^{*} = h \sum_{X,i} D_{AX(i\mp1)}^{*} \left[\frac{m}{n_{\mathrm{INT}}}\right]^{\mp i+1} \tag{32}$$

For p-type material $m = p$ and the bottom of the double sign applies, for n-type $m = n$ and the top is applicable. The prefactor h has values between 1.00 for $C_A \ll n_{\mathrm{INT}}$ and 2.00 for $C_A \gg n_{\mathrm{INT}}$.

For Si experiments show that for the common dopants, $|i| \le 2$ in Eq. (32); and that

$$D_A^{(i\mp1)^*} = \sum_X D^{*}{}_{AX(i\mp1)}$$

can be described by a single activation energy. Appropriate values are listed in Table 1 (11).

In a nonequilibrium situation, in which $C_{X^{(i\mp1)}} \neq C_{X^{(i\mp1)}}^{*}$, Eq. (30) becomes with Eq. (31)

$$\vec{J} = -\sum_{X,i} h D_{AX(i\mp1)}^{*} \frac{C_{X(i\mp1)}^{INT}}{C_{X(i\mp1)}^{INT*}} \left[\frac{m}{n_{\mathrm{INT}}}\right]^{\mp i+1} \vec{\nabla} C_A \tag{33}$$

that is, the macroscopic diffusion coefficient is now proportional to the super- or supra-saturation of the various point defects:

$$D_A = h \sum_{X,i} D_{AX(i\mp1)}^{*} \frac{C_{X(i\mp1)}^{INT}}{C_{X(i\mp1)}^{INT*}} \left[\frac{m}{n_{\mathrm{INT}}}\right]^{\mp i+1} \tag{34}$$

With Si there are only two native point defects, vacancies ($X = V$) and self-interstitials ($X = I$). The fractional intersti-

Table 1. Prefactors $D_0^{(i\mp1)}$ in units of cm²s⁻¹ and activation energies $E_a^{(i\mp1)}$ in units of eV for bulk diffusion in Si under equilibrium conditions. The index *i* represents the charge state of the dopant point defect pair.

	Element	$D_0^{(0)}$	$E_a^{(0)}$	$D_0^{(1)}$	$E_a^{(1)}$	$D_0^{(-1)}$	$E_a^{(-1)}$	$D_0^{(-2)}$	$E_a^{(-2)}$
p-type	B	0.037	3.46	0.76	3.46				
	Al	1.385	3.41	2480	4.20				
	Ga	0.374	3.39	28.5	3.92				
	In	0.785	3.63	415	4.28				
n-type	P	3.85	3.66			4.44	4.00	44.2	4.37
	As	0.066	3.44			12.0	4.05		
	Sb	0.214	3.65			15.0	4.08		

Table 2. The Interstitial Fraction of Diffusivity in Si

Dopant	B	Al	Ga	P	As	Sb
f_I	>0.98	0.6–0.7	0.6–0.7	~1	0.2–0.5	<0.012

tial component of diffusion under equilibrium conditions is defined as

$$f_{AI} = \frac{D^*_{AI}}{D^*_{AI} + D^*_{AV}} \tag{35}$$

and for intrinsic Si

$$D^*_A = D^*_{AI} + D^*_{AV} \tag{36}$$

and

$$D_A = D^*_{AI}\frac{C_I}{C^*_I} + D^*_{AV}\frac{C_V}{C^*_V} = f_{AI}\frac{C_I}{C^*_I}D^*_A + (1 - f_{AI})\frac{C_V}{C^*_V}D^*_A \tag{37}$$

Interstitial fractions have been determined experimentally for the most common dopants in Si [Table 2; (from Ref. 12; values for B and Sb from Ref. 13)]. Boron and P are thus to a high degree of accuracy pure interstitial(cy) diffusers, whereas Sb diffuses exclusively by vacancies. Boron and Sb are used as tracers of native point defects in Si, since their diffusivities are proportional to the concentration of Si self-interstitials and vacancies, respectively (1).

NONEQUILIBRIUM DIFFUSION

Transient Enhanced Diffusion

Transient enhanced diffusion (TED) is the experimental observation that interstitial diffusers such as B or P show an enhancement of diffusion during post-implantation annealing that can easily exceed a factor of 1000. The enhancement is temporary, hence the name "transient". In addition, dopant clustering occurs below the solid solubility, which is also transient, albeit with a much longer time constant. TED is observable over distances, that is, the implantation of As enhances the diffusion of already implanted and annealed boron even if the profiles do not overlap. The diffusion distances due to TED are typically on the order of 100 nm or less. Hence, the effect has become noticeable only recently, when device dimensions reached the submicron regime. In the deep submicron regime, TED dominates the redistribution of dopants and is at the center of any attempt to model dopant distributions predictively.

Medium Energy Ion Implantation with Nonamorphizing Doses. The physical mechanisms of TED depend are best understood for medium energy ion implantation (defined here as ~40 keV Si or equivalent range) at nonamorphizing doses. The salient experimental observations are:

1. The diffusion enhancement is approximately constant up to a characteristic time (*completion time*.)
2. The enhancement is approximately independent of implant energy or dose.
3. The completion time increases with energy and dose.
4. There is no TED of vacancy-mediated diffusers, that is, there is no observable vacancy supersaturation.
5. Implants enhance the diffusion of interstitial diffusers that are spatially separated from the region of implant damage.

The physical mechanisms that stand behind these observations can be summarized as follows (10,14):

1. The Frenkel pairs (Si self-interstitial and Si-vacancy) that each implanted ion creates are annihilated very quickly: Only one interstitial from the implanted ion, as it becomes substitutional, remains. This is known as the +1-model.
2. The "+1"-interstitials agglomorate into extended defects such as {311}s (15) or Boron-interstitial clusters (16).
3. The interstitial clusters dissolve, setting up an approximately constant supersaturation of interstitials that is independent of the initial implant dose and energy. TED is driven by the interstitials that "evaporate" from the clusters. The larger the dose, the more interstitials are in clusters, the longer it takes for them to dissolve, and the longer TED lasts.
4. Evaporated interstitials diffuse into the bulk or to the surface.

A simple, first-order model of cluster evaporation and dissolution describes experiments very well (17). The square of the diffusion distance of B due to TED is given by

$$\Delta x_j^{\,2} \propto R_p N_{2D} e^{-(-E_{SD}+E_{DB})/kT} \tag{38}$$

where E_{SD} = 4.9 eV is the activation energy of Si self-diffusion and E_{DB} = 3.46 eV that of B diffusion. TED thus has a negative activation energy, that is the larger the annealing temperature, the smaller the amount of diffusion due to TED.

Following implantation, substitutional dopants may become electrically inactive and immobile. The detailed physical mechanisms of this phenomenon are still under debate. Pelaz and others have presented an atomistic model involving the formation of B-cluster precursors, which describes many of the experimental observations (18).

High-Energy and Low-Energy Ion Implantation at Nonamorphizing Doses. Research into TED after high energy (HEI, energies $\gtrsim$ 100 keV Si and equivalent range) and low energy (LEI, energies $\lesssim$ 10 keV Si and equivalent range) ion implants is still at a nascent stage. On the part of HEI, such research is encouraged by the fairly recent development to form tubs (wells) during CMOS processing via ion implantation ("Profiled tub") rather than by the conventional solid state diffusion ("drive-in"). For LEI, the motivation stems from the continuing shrinkage of devices and the concomitant reduction in source/drain-junction depths to less than 50 nm for sub-100 nm gate lengths. Nevertheless a few key observations can be made: HEI leads to TED of Sb in addition to TED of B, that is, a significant amount of vacancies escape the annihilation of the Frenkel pairs (19). Agarwal and others have demonstrated that junction depth follows the implant range

dependence of Eq. (38) for Si implants down to 0.5 keV (20). To a certain extent, the same is true for B implants (21), however, a finite B diffusion enhancement exists even when the implant damage is negligible, possibly related to the formation of a B_xSi_{1-x} alloy (22). Because the small range of a typical implant for ultrashallow junction formation (0.5 keV B, 1×10^{15} cm^{-2}), the volume concentration of a dopant after implantation can exceed 10^{21} cm^{-3}, or 2%.

Transport. The transport, or diffusion of interstitials, has arguably been the largest enigma in the field of point defects. The basic difficulty for more than two decades has been the vastly differing values that have been reported for D_I, for instance, at 800°C differences of more than six orders of magnitude. It has become clear now that interstitial traps reduce D_I to an effective value much below that of a trap-free material. The strongest candidate for those traps is substitutional carbon. While this model reconciles most of the experimental data (23), the details of the mechanism, the possible role of oxygen, and the kinetics are poorly or not at all understood.

Amorphizing Implants. As a first approximation, it is often assumed that the damage that exists in the amorphous region does not give rise to TED. Only the interstitials in the tail region of the implant contribute to TED, where the volume concentration of the damage is sufficiently small so that amorphization has not occurred. Therefore, TED should saturate as the implant dose is increased above the amorphization dose. This, however, neglects the influence that the formation and dissolution of extended defects at the amorphous crystalline interface has on the native point defects (24,25).

Effects of Annealing Ambient and Thin Films on Si Point-Defects

Oxidation. Annealing of Si in dry oxygen leads to an injection of interstitials, that is, an enhancement of B- or P-diffusivity (Oxidation Enhanced Diffusion, OED). The enhancement is on the order of 10 and depends sublinearly on oxidation rate with a power law coefficient between 0.2–0.3 for thin oxides. The lower the oxidation temperature, the larger OED is. No generally accepted, atomistic model exists for the mechanism of interstitial injection during OED. The exact dependence of OED on temperature and time are still an active area of research: For a review see Refs. 13 and 26. Oxidation also leads to an undersaturation of vacancies, that is, a retardation of Sb diffusion (Oxidation Retarded Diffusion, ORD), either by recombination of vacancies with the supersaturated interstitials or by changing the equilibrium surface concentration of vacancies. Assuming the former case, the time dependence of the recombination process has been utilized to obtain an estimate for the I–V recombination time (27). The experimental result indicates the existence of an enthalpy barrier of 1.4 eV, which implies that I–V recombination is a very slow process, and that at equilibrium it takes years at temperatures of the order 800°C.

Nitridation. Nitridation in NH_3 yields an enhancement of Sb diffusion (Nitridation Enhanced Diffusion, NED) of the order 5 at temperatures of 810 to 910°C, that is, a supersaturation of vacancies, while retarding the diffusion of B or P (Nitridation Retarded Diffusion, NRD) by about the same amount, that is, an undersaturation of interstitials (28). Even less consensus exists about the physical mechanisms and the time- and temperature-dependence than in the case of OED/ORD. The available experimental data up to 1989 has been reviewed by Fahey and others (13). More recent experiments have been cited in Ref. 28.

Silicidation. Wildly varying determinations of the point defect perturbance attributed to the growth of Ti-silicides have been reported. It is now quite clear that they have to be attributed to the difficulties associated with depth profiling through the rough interface that silicidation produces. Herner and others have demonstrated that careful surface preparation after Ti- and Co-silicidation and before dopant depth profiling yields reproducible results (29): Vacancy supersaturations are quite small, of the order 2 at temperatures between 800 and 850°C, with interstitial undersaturations of the same amount, for both Co- and Ti-silicides. The observed point defect perturbance is independent of diffusing species or thickness of the film (30), that is, it is not due to strain, but its actual physical mechanism is unknown. A review of the effect of other silicides can be found in Ref. 26.

Vacuum Annealing. Under sufficiently low partial pressures of oxygen ($\lesssim 10^{-3}$ Torr at 800°C), SiO_2 is unstable and decomposes according to $Si + SiO_2 \rightarrow 2SiO$ and subsequent desorption of the volatile SiO. Similarly, oxygen in the background gas does not oxidize exposed Si to SiO_2, but only to SiO. The net effect of this reaction is etching of the underlying Si. These conditions lead to undersaturation of interstitials at 800°C, while leaving the vacancy concentration unchanged (31).

Anomalous Diffusion Phenomena of Dopants in Si

The Influence of High Concentrations. At dopant concentrations exceeding $\approx 2 \times 10^{20}$ cm^{-3}, As and Sb diffusivities increase steeply with the fourth power of the concentration, while the enthalpy of diffusion becomes only abut 2.7 eV (32) (compare with Table 1). This is understood as a cooperative phenomenon due to "sharing of vacancies" between different dopant atoms.

If the concentration of a dopant exceeds a certain, temperature-dependent value, the "solid solubility," the excess will come out of solution and form precipitates. Values for the solid solubility can be found in Ref. 7. Precipitation is not instantaneous and large supersaturations can be sustained for extended periods of time (33–35); simulations need to take the kinetics of precipitation into account (33,34).

Phosphorus. The diffusion of phosphorus above the intrinsic carrier concentration exhibits an "anomalous" behavior that manifests itself in a "kink and tail" profile as well as an enhancement of B diffusion and a retardation of Sb diffusion, both spatially separated from the P-doped region. The effect has been known since the 60s, when bipolar transistors were fabricated with P emitters and B bases: The observed large diffusion in the base is known as "emitter-dip" or "emitter-push" effect (36). The most likely cause is the "kick-out" reaction, in which an interstitial P atom kicks out a Si self-interstitial according to $P_i \leftrightarrow I + P_s$. However, the whole issue is far from settled, and numerous difficulties and inconsistencies in the interpretation of the data remain. For a review of experimental data and models see Refs. 13 and 26.

Dopant-Dopant Interactions. Dopants influence each other not only via compensation of electrical charges and the resulting changes in the Fermi level, but also by explicit interactions. This can manifest itself in changes in the solubility, as for B and Ge (37), or in the formation of pairs that may [e.g., As_2B, (38)] or may not [e.g., SbB, (39)] be electrically active. Codiffusion always modifies the diffusivities compared to the values for the single species (40), possibly even leading to uphill diffusion (41).

Boron Penetration. Boron from the p-type gate-electrode diffuses through the gate-oxide layer and into the channel region of the device during the dopant activation anneal, resulting in interface degradation and threshold voltage shifts. Krisch et al. (42) have successfully described this behavior by treating the gate-stack as a two-boundary-system (poly-silicon–oxide-silicon) and solving for the steady-state diffusion assuming that the poly-silicon is a constant source of B. Boron penetration increases exponentially as gate-oxide thickness decreases so that for sufficiently thin oxides small variations in its thickness can lead to a large spread in threshold voltages. The amount of B penetration is also dependent on the environment: F, as from a BF_2 implant, enhances it (43,44), while N incorporation in the oxide reduces B penetration (45,46). The model in Ref. 42 includes the atomistic mechanisms of B diffusion in the oxide implicitly by defining an effective diffusion distance of B in the oxide. No consensus exists about the actual physics of B diffusion in SiO_2.

Diffusion in Amorphous and Polycrystalline Materials

Diffusion during front-end processing largely takes place in single-crystalline material. However, this is not true for diffusion during back-end processing and during actual device operation. Issues such as grain-boundary diffusion ("pipe diffusion"), diffusion barriers, grain ripening, oxide and nitride growth, electro-migration, or the thermal stability of metal-alloys (solders, for example) play an important role. To give those topics justice is not possible in this space. Instead the reader is referred to the articles that can be found in Ref. 47 and 48.

BIBLIOGRAPHY

1. H.-J. Gossmann, *Dopant Diffusion and Segregation in Delta-Doped Silicon Films, in Delta-Doping of Semiconductors,* E. F. Schubert, ed., Cambridge, UK: Cambridge Univ. Press, 1996, p. 253.
2. J. Crank, *The Mathematics of Diffusion,* Oxford, UK: Clarendon Press, 1975.
3. M. R. Pinto, D. M. Boulin, C. S. Rafferty, R. K. Smith, W. M. Coughran, Jr., I. C. Kizilyalli, and M. J. Thoma, Three-dimensional characterization of bipolar transistors in a submicron BiCMOS technology using integrated process and device simulation, *Proc. IEDM,* **92**: 923, 1992.
4. M. E. Law, C. S. Rafferty, and R. W. Dutton, New n-well fabrication techniques based on 2d process simulation, *Proc. IEDM,* **86**: 518–521, 1986.
5. H. Y. Park, K. S. Jones, and M. E. Law, A point defect based two-dimensional model of the evolution of dislocation loops in silicon during oxidation, *J. Electrochem. Soc.,* **141**: 759–765, 1994.
6. Landolt-Börnstein, *Zahlenwerte und Funktionen aus Naturwissenschaft und Technik,* Vol. 17c, O. Madelung, M. Schulz, and H. Weiss, eds. (Springer, Berlin, 1984).
7. Landolt-Börnstein, *Zahlenwerte und Funktionen aus Naturwissenschaft und Technik,* Vol. 22b, O. Madelung and M. Schulz, eds. (Springer, Berlin, 1989).
8. P. M. Fahey, P. B. Griffin, and J. D. Plummer, Point defects and dopant diffusion in silicon, *Rev. Mod. Phys.,* **61**: 289, 1989.
9. F. J. Morin and J. P. Maita, Electrical Properties of silicon containing arsenic and boron, *Phys. Rev.,* **96**: 28–35, 1954.
10. C. S. Rafferty, Progress in predicting transient diffusion, *Int. Conf. Simulation Semi. Proc. Dev.,* Cambridge, MA: IEEE, p. 1, 1997.
11. R. B. Fair, in *Impurity Doping Processes in Silicon,* F. F. Y. Wang, ed., Amsterdam: North Holland, 1981, ch. 7.
12. U. Gösele and T. Y. Tan, The nature of point defects and their influence on diffusion processes in silicon at high temperatures, *Proc. Mater. Res. Soc.,* **14**: 45, 1982.
13. H.-J. Gossmann et al., The interstitial fraction of diffusivity of common dopants in silicon, *Appl. Phys. Lett.* **71**: 3862, 1997.
14. P. A. Stolk et al., Physical mechanisms of transient enhanced dopant diffusion in ion-implanted silicon, *J. Appl. Phys.,* **81**: 6031, 1997.
15. D. J. Eaglesham et al., Implantation and transient B diffusion in Si: The source of the interstitials, *Appl. Phys. Lett.,* **65**: 2305, 1994.
16. L. H. Zhang et al., Transient enhanced diffusion without {311} defects in low energy B^+ implanted silicon, *Appl. Phys. Lett.,* **67**: 2025, 1995.
17. C. S. Rafferty et al., Simulation of cluster evaporation and transient enhanced diffusion in silicon, *Appl. Phys. Lett.,* **68**: 2395, 1996.
18. L. Pelaz et al., B Diffusion and Clustering in Ion Implanted Si: The Role of B Cluster Precursors, *Appl. Phys. Lett.,* **70**: 2285, 1997.
19. D. J. Eaglesham et al., Transient enhanced diffusion of Sb and B due to MeV silicon implants, *Appl. Phys. Lett.,* **70**: 3281, 1997.
20. Aditya Agarwal et al., Reduction of transient enhanced diffusion from 1–5 keV Si^+ implantation due to surface annihilation of interstitials, *Appl. Phys. Lett.,* **70**: 3332, 1997.
21. J. Liu et al., The Effect of Boron Implant Energy on Transient Enhanced Diffusion in Silicon, *J. Appl. Phys.,* **81**: 1656, 1997.
22. Aditya Agarwal et al., Boron-Enhanced-Diffusion of Boron: The limiting factor for ultra-shallow junctions, *IEDM Tech. Dig.,* p. 467, 1997.
23. H.-J. Gossmann and J. M. Poate, Dopant and Intrinsic Point-Defect Interactions in Si, *Proc. 23rd Int. Conf. Phys. Semicond.,* **4**: 2569, Singapore: World Scientific, 1996.
24. J. K. Listebarger et al., Study of end of range loop interactions with B^+ implant damage using a boron doped diffusion layer, *J. Appl. Phys.,* **78**: 2298–2302, 1995.
25. H. S. Chao et al., Species and dose dependence of ion implantation damage induced transient enhanced diffusion, *J. Appl. Phys.,* **79**: 2352–2363, 1996.
26. S. M. Hu, Nonequilibrium point defects and diffusion in silicon, *Mater. Sci. Eng.,* **R13**: 103–192, 1994.
27. D. A. Antoniadis and I. Moskowitz, Diffusion of substitutional impurities in silicon at short oxidation times: An insight into point defect kinetics, *J. Appl. Phys.,* **53**: 6788–6796, 1982.
28. T. K. Mogi et al., Thermal nitridation enhanced diffusion of Sb and Si(100) doping superlattices, *Appl. Phys. Lett.,* **69**: 1273, 1996.
29. S. B. Herner et al., Point defects in Si after formation of a $TiSi_2$ film: evidence for vacancy supersaturation and interstitial depletion, *Appl. Phys. Lett.,* **68**: 1687, 1996.

30. S. B. Herner et al., The influence of $TiSi_2$ and $CoSi_2$ growth on Si native point defects: the role of the diffusing species, *Appl. Phys. Lett.,* **68**: 2870, 1996.
31. H.-J. Gossmann et al., Behavior of Intrinsic Si Point Defects During Annealing in Vacuum, *Appl. Phys. Lett.,* **67**: 1558, 1995.
32. A. Nylandsted Larsen et al., Heavy doping effects in the diffusion of group IV and V impurities in silicon, *J. Appl. Phys.,* **73**: 691, 1993.
33. S. Solmi, E. Landi, and F. Baruffaldi, High-concentration boron diffusion in silicon: Simulation of the precipitation phenomena, *J. Appl. Phys.,* **68**: 3250, 1990.
34. S. Solmi, F. Baruffaldi, and M. Derdour, Experimental investigation and simulation of Sb diffusion in Si, *J. Appl. Phys.,* **71**: 697, 1992.
35. H.-J. Grossmann, F. C. Unterwald, and H. S. Luftman, Doping of Si thin films by low temperature molecular beam epitaxy, *J. Appl. Phys.,* **73**: 8237, 1993.
36. L. E. Miller, *Properties of Elemental and Compound Semiconductors,* H. Gato (ed.), New York: Interscience, 1960, 303.
37. P.-E. Hellberg et al., Boron-doped poly-crystalline Si_xGe_{1-x} films, *J. Electrochem. Soc.,* **144**: 3968, 1997.
38. K. Yokota et al., Interactions between arsenic and boron implanted in silicon during annealing, *J. Appl. Phys.,* **69**: 2975, 1991.
39. R. B. Fair, M. L. Manda, and J. J. Wortman, The diffusion of antimony in heavily doped and n- and p-type silicon, *J. Mat. Res.,* **1**: 705, 1986.
40. S. Solmi and S. Valmorri, Codiffusion of arsenic and boron implanted in silicon, *J. Appl. Phys.,* **77**: 2400, 1995.
41. J. Bevk et al., *Method for making a semiconductor device including diffusion control,* US Patent No. 5500391.
42. K. S. Krisch et al., Thickness dependence of boron penetration through O_2 and N_2O-grown gate oxides and its impact on threshold voltage variation, *IEEE Trans. Electron. Devices,* **43**: 982, 1996.
43. F. K. Baker et al., The influence of fluorine on threshold voltage instabilities in p^+ polysilicon gate p-channel MOSFETs, *IEDM Tech. Dig.,* **89**: 443, 1989.
44. J. M. Sung et al., Fluorine effect on boron diffusion of p^+ gate devices, *IEDM Tech. Dig.,* **89**: 447, 1989.
45. S. S. Wong et al., Low pressure nitrided-oxide as a thin gate dielectric for MOSFETs, *J. Electrochem. Soc.,* **130**: 1139, 1983.
46. A. B. Joshi, J. Ahn, and D. L. Kwong, Oxynitride gate dielectrics for p^+-polysilicon gate MOS devices, *IEEE Electron Dev. Lett.,* **14**: 560, 1993.
47. D. Gupta and P. S. Ho, *Diffusion phenomena in thin films and microelectronic materials,* Park Ridge, NJ: Noyes, 1988.
48. G. E. Murch and A. S. Nowick, *Diffusion in Crystalline Solids,* New York: Academic, 1984.

HANS-JOACHIM L. GOSSMANN
Bell Laboratories, Lucent Technologies

DIFFUSION. See ACTIVATION ENERGY.

DIFFUSION, SEMICONDUCTOR. See SEMICONDUCTOR DOPING.